ChemComm

Cite this: *Chem. Commun.*, 2011, **47**, 10713–10715

www.rsc.org/chemcomm

COMMUNICATION

A novel pH-sensitive (±)-α-tocopherol–5-fluorouracil adduct with antioxidant and anticancer properties†

Dong-Wei Li,[a] Fang-Fang Tian,[a] Yu-Shu Ge,[a] Xin-Liang Ding,[a] Jia-Han Li,[a] Zi-Qiang Xu,[a] Mei-Fang Zhang,[a] Xiao-Le Han,[a] Ran Li,[a] Feng-Lei Jiang[a] and Yi Liu*[ab]

Received 27th June 2011, Accepted 24th August 2011
DOI: 10.1039/c1cc13821a

A novel pH-sensitive (±)-α-tocopherol–5-fluorouracil (VE-5-FU) adduct with antioxidant and anticancer properties for antioxidant-based cancer chemoprevention was synthesized and utilized for selective drug release in the stomach.

Cancer, aging, atherosclerosis, and some other serious diseases have been confirmed to correlate with low density lipoprotein (LDL), cell membranes, and DNA exposed to oxidative stress.[1] It is generally believed that the formation of growth promoting oxidants (reactive oxygen species, ROS) is a major "catalyst" of the tumor promotion and progression stages.[2] ROS involve a series of oxidants, such as hydrogen peroxide (H_2O_2), singlet oxygen ($^1O_2$), free radicals ($DPPH^{\bullet}$), *etc.*, among which the radicals attract much attention because they can drive carcinogenesis by damaging DNA and proteins.[3] Thus, some works are devoted to investigating the radical-scavenging properties of the presented anticancer drugs to enlarge the application of these drugs as antioxidants.[4] However, the antioxidant–anticancer hybrid as a dual-acting drug has been seldom reported up to now.

Recently, stimuli-responsive drugs have attracted more and more attention for controlling the release rate and targeting the release site, because the release can be triggered by environmental temperature, pH and/or light.[5] Among those drugs, pH-responsive drugs have been paid much attention because of large variations in physiological pH at different body sites under normal as well as pathological conditions.[6] For example, the pH value of the human body increases from the stomach (pH 1.0–3.0) to the small intestine (pH 6.5–7.0), and to the colon (pH 7.0–8.0).[7] The most common strategy for facilitating the pH-responsive controllable release is the use of synthetic polymer–drug conjugates.[5b,c] One significant limitation of this strategy, however, is the use of an exogenous polymer, metabolism and excretion of which in the body is still an urgent problem. Thus, the application of a natural molecule as the drug carrier would be a promising strategy to solve this problem.

α-Tocopherol, the most active component of natural vitamin E, consists of a chromanol head, which is located at the water–lipid interface, and a long saturated phytyl chain tail, which is buried within the hydrocarbon chains in the lipid bilayers.[8] The structure of α-tocopherol affords its ease of incorporation into membranes, which might facilitate the transport of conjugates into the interior of cancer cells.[9] The antioxidant activity of α-tocopherol relies on its effectiveness in donating hydrogen from the hydroxyl group of the chromanol ring to reactive radicals,[10] so when α-tocopherol exists in the form of an ester conjugate the antioxidant activity will be hidden (as shown in Scheme 1). Based on these properties, we report herein (to the best of our knowledge) the first pH-sensitive (±)-α-tocopherol–5-fluorouracil conjugate (**VE-5-FU**) as a dual-acting drug (antioxidant–anticancer) for antioxidant-based cancer chemoprevention, which can hold the conjugate form at a higher pH value (pH 7.0–8.0) and release the two single units at a lower pH value (pH 1.0–3.0). This dual-acting adduct could have potential application for delivering the bifunctional drug to the target site of lower pH value, such as the stomach. Additionally, the systematic biophysical investigation of the interaction between serum albumin (SA) and **VE-5-FU** is also discussed, as the absorption, distribution, and metabolism of drugs are strongly dependent on the interactions between SA and drugs.

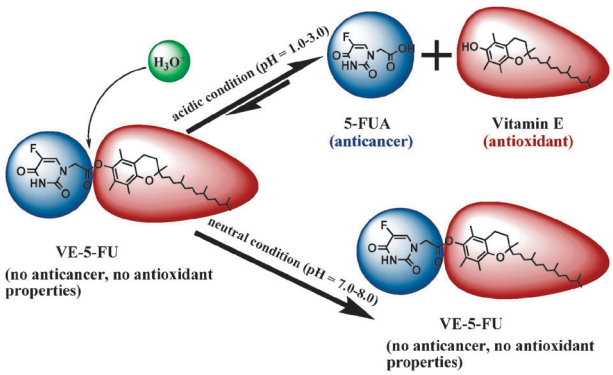

Scheme 1 Schematic representation of the **VE-5-FU** acid-triggered drug release process. The 5-FUA (blue) and Vitamin E (red) are highlighted in the scheme.

[a] *State Key Laboratory of Virology & Key Laboratory of Analytical Chemistry for Biology and Medicine (MOE), College of Chemistry and Molecular Sciences, Wuhan University, Wuhan 430072, P. R. China. E-mail: yiliuchem@whu.edu.cn; Fax: +86-27-6854067; Tel: +86-27-68756667*
[b] *Department of Chemistry and Life Sciences, Xianning University, Xianning 437005, P. R. China*

† Electronic supplementary information (ESI) available. See DOI: 10.1039/c1cc13821a

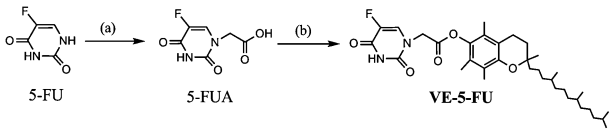

Scheme 2 The synthesis route for **VE-5-FU**. (a) $ClCH_2COOH$, KOH, refluxed, 2 h; (b) (±)-α-tocopherol, DCC/THF, Ar, 50 °C, stirred, 48 h.

The coupling of the two segments to obtain the conjugate **VE-5-FU** was done using general ester synthesis techniques (Scheme 2), and the radical-scavenging properties of **VE-5-FU** were tested in a semi-aqueous system using 2,2-diphenyl-1-picrylhydrazyl ($DPPH^{\bullet}$) as a radical species (for details and characterization see ESI†). Generally, when **VE-5-FU** was added to a deaerated EtOH–H_2O (1 : 1) solution of $DPPH^{\bullet}$ at different pH (pH 1.0–8.0), the visible absorption band at 525 nm due to $DPPH^{\bullet}$ disappeared gradually, indicating that the $DPPH^{\bullet}$-scavenging reaction of **VE-5-FU** was taking place. In those cases in which pH = 1.0, the $DPPH^{\bullet}$ radical was unstable, so the measurement of the scavenging property at pH = 1.0 was imprecise. As illustrated in Fig. 1a, the radical-scavenging properties of **VE-5-FU** were time- and pH-dependent. Under the neutral conditions (pH = 7.0–8.0), the $DPPH^{\bullet}$ capture behavior of **VE-5-FU** was relatively weak, with the majority (>90%) of $DPPH^{\bullet}$ remaining for 5 h. However, $DPPH^{\bullet}$-scavenging was much enhanced at pH of 2.0, and over 55% of the initial $DPPH^{\bullet}$ was scavenged within 5 h, due to highly efficient hydrolysis of the acid-sensitive **VE-5-FU** ester conjugate. To optimize the reaction conditions, radical-scavenging properties with different **VE-5-FU** concentrations are also discussed, as shown in Fig. 1b, which indicated that we had the chance to optimize our drug system by using higher **VE-5-FU** concentrations.

To assess the anticancer activity of **VE-5-FU** and 5-FUA directly, the cell viability of the human cervical cancer HeLa cell line was monitored by the MTT assay. The results of cell viability of **VE-5-FU** and its precursor 5-FUA are shown in Fig. 2. Based on the MTT results, the enhancement of cytotoxicity for **VE-5-FU** compared to 5-FUA indicated that the cell membrane-permeable α-tocopherol moiety might facilitate the transport of conjugates into the interior of cancer cells. Moreover, the acidic intracellular compartments such as endosomes (pH 5.0–6.0) and lysosomes (pH 4.0–5.0) might also trigger the release of **VE-5-FU**.

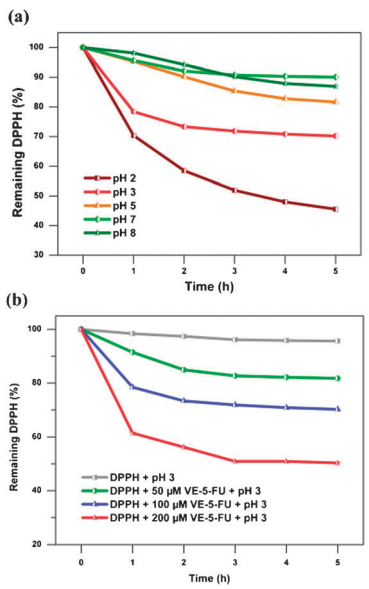

Fig. 1 (a) The $DPPH^{\bullet}$-scavenging properties of **VE-5-FU** in semi-aqueous solutions at rt at pH 2, 3, 5, 7, 8. The concentrations are 50 μM for $DPPH^{\bullet}$, and 100 μM for **VE-5-FU**, respectively. (b) The effect of **VE-5-FU** concentration on $DPPH^{\bullet}$-scavenging properties.

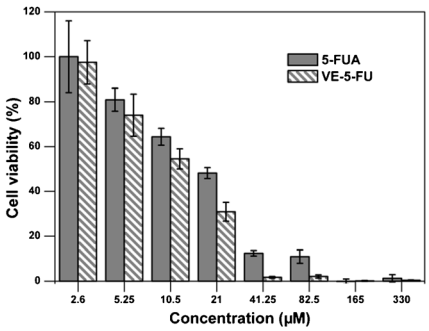

Fig. 2 *In vitro* cell assays of 5-FUA and **VE-5-FU** against HeLa cells. Cells incubated with drugs at different concentrations (2.6–330 μM) at 37 °C for 48 h.

It is widely accepted in the pharmaceutical industry that an understanding of the chemistry of the various classes of pharmaceutical interactions with SA can suggest new approaches to drug therapy and design.[11] We first studied the influence of **VE-5-FU** on the binding affinity and secondary structure of SA. The Stern–Volmer quenching constants (K_{SV}) for **VE-5-FU**–SA and 5-FUA–SA systems were $1.223 \times 10^4\ M^{-1}$ and $1.492 \times 10^4\ M^{-1}$, respectively (see Fig. S3 in ESI†). Obviously, there were no significant changes in K_{SV} for **VE-5-FU** compared to its precursor 5-FUA, which illustrated that the derivatization of the traditional anticancer drug 5-FUA had almost no influence on the binding affinity of the drug–SA system. As shown in CD spectra (see Fig. S4 in ESI†), the contents of α-helix, β-sheet and unordered calculated by SELCON3 suggested that the binding of **VE-5-FU** to SA had no significant impact on the secondary structure of SA, and therefore, **VE-5-FU** could be successfully carried by SA without detriment to the function of SA.

We then investigated the affinity constant (K_A) and binding site of the **VE-5-FU**–SA system *via* experimental and theoretical methods. The results of UV-vis absorption spectra (see Fig. S5 in ESI†) confirmed that the probable binding mechanism of **VE-5-FU** to SA was a complex formation process, rather than a collision process. Thus, we could use the electrochemical impedance spectroscopy (EIS) experiment to obtain K_A for the **VE-5-FU**–SA complex.[12] Comparing the EIS of a bare Au electrode with that of a SA-modified Au electrode, R_{ct} (the diameter of the semicircle of the Nyquist plot) increased strikingly after deposition of SA (Fig. 3a). This should be attributed to the blocking of electron transport after deposition of SA on the Au surface (Fig. 3b). Fig. 3c clearly shows that R_{ct} increased with increasing concentrations of **VE-5-FU** solutions. According to the Langmuir adsorption isotherm:

$$R_{ct} = (R_{ct})_{max} C_0 K_A / (1 + C_0 K_A)$$

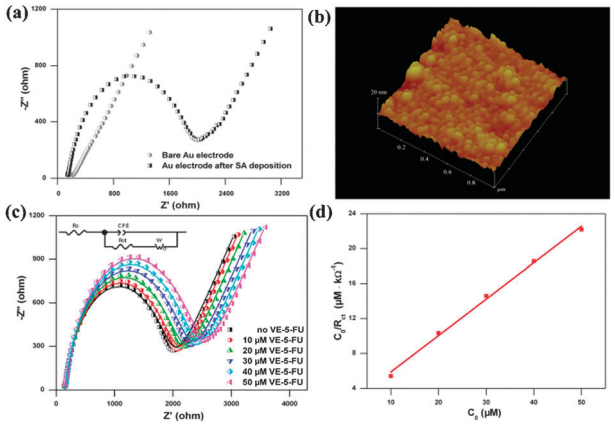

Fig. 3 (a) Nyquist plots of impedance spectra recorded for the Au electrode before and after SA deposition. (b) AFM image (recorded in the tapping mode) of the Au surface after deposition of SA. Structures with lateral dimensions in the range of 41–57 nm and a height of up to 8 nm are seen. These are not compatible with dimensions of single SA obtained from the X-ray crystallography (18.3 nm × 9.5 nm for the in-plane dimensions and 3.8 nm for the height of SA). These structures indicate the formation of aggregates, possibly due to nonspecific protein binding. (c) Nyquist plots for impedance measurements corresponding to the SA modified Au electrode with different **VE-5-FU** concentrations. Dotted symbols represent experimental data; solid lines show the curves fitted to the equivalent circuit (the inset) with best parameters. (d) Linear plot of the Langmuir isotherm of the data presented in (c).

a plot of C_0/R_{ct} as a function of C_0 yielded a straight line from which the affinity constant $K_A = 2.47 \times 10^5\ M^{-1}$ was deduced as shown in Fig. 3d. It showed that the binding constant between **VE-5-FU** and SA was moderate, and **VE-5-FU** could be stored and carried by this protein in the body.

According to Sudlow's nomenclature, two primary sites (I and II) have been identified for ligands binding to SA. The identification of the binding site of **VE-5-FU** in SA was studied by two different methods. The first method was a site marker competitive experiment, which was carried out by using warfarin and ibuprofen as site marker fluorescence probes for monitoring sites I and II of SA, respectively. The results of the site marker competitive experiment indicated that the binding site of **VE-5-FU** was mainly located within site I of SA (see Fig. S6 in ESI†). A second method, Surflex-Dock program, which was developed by Jain,[13] simulated the exact binding conformation between **VE-5-FU** and SA. As shown in Fig. 4a, site I was suggested as the main binding location since

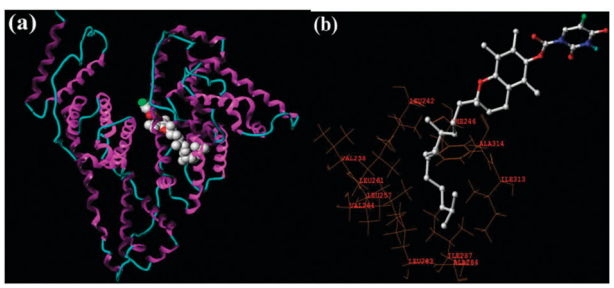

Fig. 4 Docking results of the **VE-5-FU**–SA system. (a) Binding site of **VE-5-FU** in SA. **VE-5-FU** is shown in a space-filling model. (b) Detailed illustration of hydrophobic residues around the phytyl chain tail of **VE-5-FU**.

the score (stands for $-\log K_d$) calculated between site I and **VE-5-FU** is much higher than that of site II, which was consistent with the site marker competitive result. The long hydrophobic chain tail of **VE-5-FU** was inserted into a hydrophobic cave created by the residues Leu242, Phe246, Ala314, Ile313, Ile287, Ala284, Leu283, Val264, Leu257, Leu261, and Val258 (Fig. 4b). One hydrogen bond had been observed in the **VE-5-FU**–SA system: O4 in the **VE-5-FU** molecule formed one hydrogen bond with the H atom in Arg218 (see Fig. S7 in ESI†). These results suggested that the main forces of **VE-5-FU**–SA interaction were hydrophobic interaction and van der Waals force, and the hydrogen bond also stabilized the formation of the **VE-5-FU**–SA complex.

In conclusion, we report herein a novel pH-sensitive (±)-α-tocopherol–5-fluorouracil (**VE-5-FU**) adduct with antioxidant and anticancer properties. This hybrid could be released in an acidic medium rather than in a neutral medium. The adduct also possesses enhanced anticancer activity against HeLa cells and moderate binding affinity to serum albumin. This dual-acting adduct could have potential application for delivering the bifunctional drug for antioxidant-based cancer chemoprevention to the target site of lower pH value, such as the stomach.

This work was supported by the financial support of the National Natural Science Foundation of China (21077081, 20921062), Program for Changjiang Scholars and Innovative Research Team in University (IRT1030), and the Fundamental Research Funds for the Central Universities (201120302020013).

Notes and references

1 (*a*) T. B. L. Kirkwood and S. N. Austad, *Nature*, 2000, **408**, 233–238; (*b*) T. Finkel and N. J. Holbrook, *Nature*, 2000, **408**, 239–247.
2 W. Ren, Z. Qiao, H. Wang, L. Zhu and L. Zhang, *Med. Res. Rev.*, 2003, **23**, 519–534.
3 (*a*) S. P. Hussain, L. J. Hofseth and C. C. Harris, *Nat. Rev. Cancer*, 2003, **3**, 276–285; (*b*) Z. Q. Liu, *Chem. Rev.*, 2010, **110**, 5675–5691.
4 (*a*) Y.-P. Qian, Y.-J. Cai, G.-J. Fan, Q.-Y. Wei, J. Yang, L.-F. Zheng, X.-Z. Li, J.-G. Fang and B. Zhou, *J. Med. Chem.*, 2009, **52**, 1963–1974; (*b*) G. Cirillo, K. Kraemer, S. Fuessel, F. Puoci, M. Curcio, U. G. Spizzirri, I. Altimari and F. Iemma, *Biomacromolecules*, 2010, **11**, 3309–3315; (*c*) H. M. Chen, Y. C. Wu, Y. C. Chia, F. R. Chang, H. K. Hsu, Y. C. Hsieh, C. C. Chen and S. S. Yuan, *Cancer Lett.*, 2009, **286**, 161–171.
5 (*a*) J. Zou, G. Jafr, E. Themistou, Y. Yap, Z. A. P. Wintrob, P. Alexandridis, A. C. Ceacareanu and C. Cheng, *Chem. Commun.*, 2011, **47**, 4493–4495; (*b*) K. T. Oh, H. Yin, E. S. Lee and Y. H. Bae, *J. Mater. Chem.*, 2007, **17**, 3987–4001; (*c*) Z. Liu, Q. Lin, Q. Huang, H. Liu, C. Bao, W. Zhang, X. Zhong and L. Zhu, *Chem. Commun.*, 2011, **47**, 1482–1484.
6 P. Gupta, K. Vermani and S. Garg, *Drug Discovery Today*, 2002, **7**, 569–579.
7 S.-H. Cheng, W.-N. Liao, L.-M. Chen and C.-H. Lee, *J. Mater. Chem.*, 2011, **21**, 7130–7137.
8 E. Niki and N. Noguchi, *Acc. Chem. Res.*, 2004, **37**, 45–51.
9 (*a*) R. Vallinayagam, J. Weber and R. Neier, *Org. Lett.*, 2008, **10**, 4453–4455; (*b*) S. H. Goh, N. F. Hew, A. W. Norhanom and M. Yadav, *Int. J. Cancer*, 1994, **57**, 529–531.
10 S. Tafazoli, J. S. Wright and P. J. O'Brien, *Chem. Res. Toxicol.*, 2005, **18**, 1567–1574.
11 (*a*) G. Zhang, B. Keita, C. T. Craescu, S. Miron, P. de Oliveira and L. Nadjo, *Biomacromolecules*, 2008, **9**, 812–817; (*b*) B. Ahmad, S. Parveen and R. H. Khan, *Biomacromolecules*, 2006, **7**, 1350–1356.
12 D. Li, X. Zou, Q. Shen and S. Dong, *Electrochem. Commun.*, 2007, **9**, 191–196.
13 (*a*) A. N. Jain, *J. Med. Chem.*, 2003, **46**, 499–511; (*b*) T. A. Pham and A. N. Jain, *J. Med. Chem.*, 2006, **49**, 5856–5868; (*c*) A. N. Jain, *J. Comput.-Aided Mol.Des.*, 2007, **21**, 281–306.